

This article was downloaded by:

On: 25 January 2011

Access details: *Access Details: Free Access*

Publisher *Taylor & Francis*

Informa Ltd Registered in England and Wales Registered Number: 1072954 Registered office: Mortimer House, 37-41 Mortimer Street, London W1T 3JH, UK



Liquid Crystals

Publication details, including instructions for authors and subscription information:

<http://www.informaworld.com/smpp/title~content=t713926090>

Bandwidth-controllable reflective cholesteric gels from photo- and thermally-induced processes

Renwei Guo^a; Hui Cao^a; Chaoyong Yang^b; Xiaojuan Wu^a; Qingyong Meng^a; Tao Liu^a; Wanli He^a; Zihui Cheng^a; Huai Yang^a

^a Department of Materials Physics and Chemistry, School of Materials Science and Engineering, University of Science and Technology Beijing, Beijing, P.R. China ^b Shaanxi Applied Physical Chemistry Institute, Shaanxi, Xian, P.R. China

Online publication date: 04 March 2010

To cite this Article Guo, Renwei , Cao, Hui , Yang, Chaoyong , Wu, Xiaojuan , Meng, Qingyong , Liu, Tao , He, Wanli , Cheng, Zihui and Yang, Huai(2010) 'Bandwidth-controllable reflective cholesteric gels from photo- and thermally-induced processes', *Liquid Crystals*, 37: 3, 311 – 316

To link to this Article: DOI: 10.1080/02678290903548869

URL: <http://dx.doi.org/10.1080/02678290903548869>

PLEASE SCROLL DOWN FOR ARTICLE

Full terms and conditions of use: <http://www.informaworld.com/terms-and-conditions-of-access.pdf>

This article may be used for research, teaching and private study purposes. Any substantial or systematic reproduction, re-distribution, re-selling, loan or sub-licensing, systematic supply or distribution in any form to anyone is expressly forbidden.

The publisher does not give any warranty express or implied or make any representation that the contents will be complete or accurate or up to date. The accuracy of any instructions, formulae and drug doses should be independently verified with primary sources. The publisher shall not be liable for any loss, actions, claims, proceedings, demand or costs or damages whatsoever or howsoever caused arising directly or indirectly in connection with or arising out of the use of this material.

Bandwidth-controllable reflective cholesteric gels from photo- and thermally-induced processes

Renwei Guo^a, Hui Cao^a, Chaoyong Yang^b, Xiaojuan Wu^a, Qingyong Meng^a, Tao Liu^a, Wanli He^a, Zihui Cheng^a and Huai Yang^{a*}

^aDepartment of Materials Physics and Chemistry, School of Materials Science and Engineering, University of Science and Technology Beijing, Beijing 100083, P.R. China; ^bShaanxi Applied Physical Chemistry Institute, Shaanxi, Xian 710061, P.R. China

(Received 11 November 2009; final version received 10 December 2009)

A bandwidth-controllable reflective gel has been investigated from photo- and thermally-induced processes. Due to the pitch of cholesteric liquid crystal (CLC) composite increasing as the temperature rises, the CLC with short pitch is frozen by UV-curing the polymer network at low temperature and the CLC with long pitch is fixed by heat curing the polymer network at high temperature. A non-uniform pitch distribution of CLCs forms in the gel when temperature becomes low. It is demonstrated that the memory effect of the polymer network is an important mechanism for the resulting gel.

Keywords: cholesteric liquid crystal; monomer; network; polymerisation

1. Introduction

The use of polymer network to stabilise and modify cholesteric liquid crystal (CLC) phases for display-based applications has recently become widespread [1–6]. A polymer-stabilised cholesteric liquid crystal (PSCLC) is generally produced by photopolymerisation of a relatively small amount of a photo-reactive, bifunctional monomer and chiral dopant dissolved in the liquid crystal. The monomers are often mesogenic themselves and often contain end-standing acrylate or methacrylate functional groups, which are polymerised through a radical-chain polymerisation in the presence of a photo initiator and illumination with ultraviolet (UV)-light. PSCLC's fabrication implies an understanding of the relationship among monomer constitution [7], polymerisation conditions [8,9], network morphology [10–14] and electro-optical performance [15,16].

Recently, much attention has been focused on non-uniform pitch distribution and polymer network in PSCLC to obtain the effect of wide-band reflection [17,18]. A UV-absorbing dye was used to create an intensity gradient of the UV-light through the thickness of a solid CLC polymer network [19,20]. Yang *et al.* [21] obtained wide-band reflective polariser, in which the bandwidth of the selective reflection spectrum of CLC becomes wider and narrower reversibly with increasing and decreasing temperature. However, the LC devices using both UV-light and heat curable monomers to frozen CLCs in the visible spectrum are less reported.

The present work developed a single-layer CLC composite cell prepared by photo-polymerisation at low temperature and heat-polymerisation at high temperature in sequence. The previous work showed that the heat curable monomers did not take part in the UV-curing process [22]. Due to the pitch of CLC composite increasing as the temperature rises, the CLCs with short pitch are frozen by UV-curing the polymer network at low temperature and the CLCs with long pitch are fixed by heat curing the polymer network at high temperature. A non-uniform pitch distribution forms in the cell when temperature changes. The location of the reflection band can be controlled through species of heat curable monomers. The mechanisms of forming non-uniform pitch distribution are studied in detail and the experiments clarifying the controllable reflection are described.

2. Experiments

2.1 Materials

In this study, nematic mesogens (SLC-1717, TN-I = 92°C, Slichem Co. Ltd), rigid chain heat curable monomers, diglycidyl ether of bisphenol F (DGEBF, EPON 862, Zhaochang Int'I Trade [Shanghai] Co. Ltd.), 4, 4'-Diamino dicyclohexyl methane (PACM, Dow Chemicals Co. Ltd), flexible chain heat curable monomers, 2, 2'-(ethylenedioxy)bis(ethylamine) (EDBEA, Alfa Aesar, Johnson Matthey Co.), ethylene glycol diglycidyl ether (EGDE, XY 669, Anhui Hengyuan Chemical Co. Ltd),

*Corresponding author. Email: yanghuai@mater.ustb.edu.cn

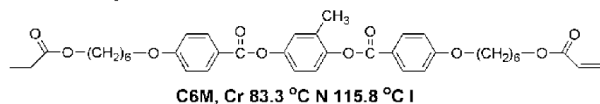
photo-polymerisable monomer, 1, 4-di-[4-(6-acryloyloxy)hexyloxy benzoyloxy]-2-methyl benzene (C6M), chiral dopant, (+)-1, 1'-binaphthyl-2, 2'-diylbis(4'-(2-methylbutyl)biphenyl-4-carboxylate) and photo-initiator, 2, 2-dimethoxy-1, 2-diphenyl-ethanone (IRG651, TCI Co. Ltd) were used. Chiral dopant above was lab-synthesised [23]. C6M was synthesised according to the method suggested by D.J. Broer [24]. Figure 1 shows the chemical structures of these materials.

Sample 1 with rigid chain heat curable monomers, Sample 2 with flexible ones and Sample 3 without heat curable monomers were prepared. The weight ratios (%) of Samples 1, 2 and 3 were SLC-1717/CD/DGEBF/PACM/C6M/IRG651 = 82.7/5.0/4.0/2.0/6.0/0.3, SLC-1717/CD/EGDE/EDBEA/C6M/IRG651 = 82.7/5.0/5.0/1.0/6.0/0.3 and SLC-1717/CD/C6M/IRG651 = 88.7/5.0/6.0/0.3, respectively.

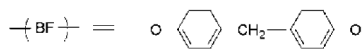
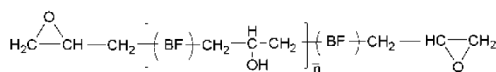
2.2 Characterisation and measurements of samples

The optical textures of samples were observed by a polarising optical microscope (POM, Olympus BX51) with a hot stage calibrated to an accuracy of $\pm 0.1^\circ\text{C}$ (LinkamTHMS-600). The differential scanning

Photo-polymerisable monomer



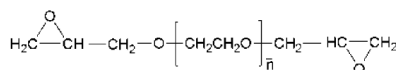
Rigid chain heat curable monomers



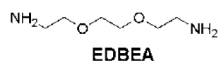
DGEBF, n=0.13

PACM

Flexible chain heat curable monomers

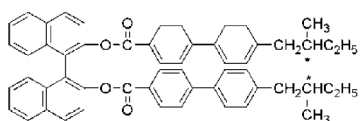


EGDE, n=3.4



EDBEA

Chiral dopant



HTP=62, Right-handed

Figure 1. Chemical structure of photo-polymerisable monomer, heat curable monomers and chiral dopant.

calorimetric (DSC, PerkinElmer Pyris 6) analysis was carried out with a heating and a cooling rate of $10^\circ\text{C min}^{-1}$ under a dry nitrogen purge. The reflection spectra were obtained by UV/VIS/NIR spectrophotometer (JASCO V-570) in reflection mode at normal incidence. The morphology of the polymer network of the PSCLCs films was studied by scanning electron microscopy (SEM, Leicas 440I). The film was first separated, dipped into n-hexane for 24 h at room temperature, and then the polymer network was dried for 12 h under a vacuum. The films were sputtered with carbon before the observation of the microstructure of the polymer network under SEM.

2.3 Preparation of the samples

The cell's two inner surfaces with polyvinyl alcohol (PVA) layers were rubbed in perpendicular directions to provide a homogeneous orientation of LC molecules. 60- μm thick polyethylene terephthalate (PET) films were used as a spacer of the cells. All the mixtures exhibited a cholesteric phase at room temperature and were filled into the cell by capillary action. The composite exhibited a planar texture when it was filled into the cell under homogeneous boundary conditions.

The PSCLC cells reflecting visible light flux range were prepared by carrying out the following procedure. At first, the cells of Samples 1, 2 and 3 were irradiated with UV-light (1.0 mW cm^{-2} , 365 nm) for 1 h at 20°C , during which a polymer network was formed from the photo-polymerisation of C6M. Following that, the cells of Samples 1 and 2 were heated in an oven for 4 h at 55°C , and the heat curable monomers formed a polymer network through heat-polymerisation. The heat curable temperature was lower than the clear point of samples. Finally, the cells were kept at room temperature.

3. Results and discussion

The phase transition temperatures of Samples 1–3 were measured by DSC as shown in Figure 2. The clear points of Samples 1–3 are 60.0, 61.6, and 76.1°C , respectively.

The sol/gel and FT-IR methods were used to determine the heat curable conditions including the reaction degree and heat curable time. Figure 3(a) shows that the gel fraction of rigid chain heat curable monomers increased with heat curing time and changed little from a value of about 94 wt% after a heat curing time of 4.0 h. In the sol/gel method, the heat monomers were coated on a glass substrate, then the heat curing process was applied. The solid film was peeled off from the glass substrate. The soluble materials in the solid films were extracted in acetone for 72 h and

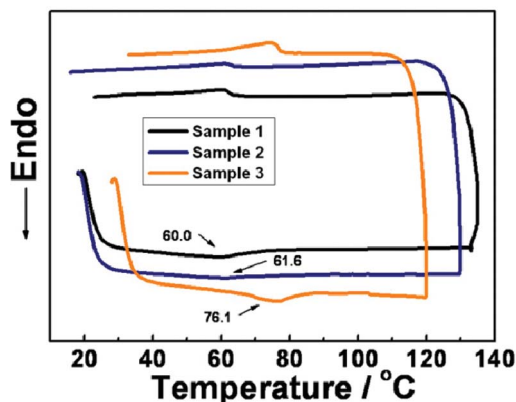


Figure 2. The DSC thermogram of Samples 1, 2 and 3 before polymerisation.

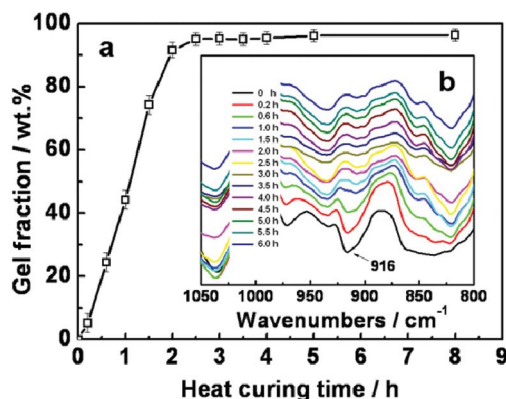


Figure 3. The rigid chain heat curable monomers. (a) The time dependence of gel fractions. (b) FT-IR curves of the reaction.

the extracted films were then dried in a vacuum at 60°C for 24 h. The gel fraction was taken as the ratio of the weight of the extracted film to that of the non-extracted one and three parallel groups of Samples were weighed to obtain an average value. In the FT-IR spectrum, an absorption peak at 916 cm^{-1} is the observed character of the epoxy ring as shown in Figure 3(b). By comparing the peak areas of epoxy ring with heat curing time increased, we concluded that it changed little after a heat curing time of about 4.0 h which indicates that 4.0 h is a suitable heat curing time of rigid chain heat curable monomers.

Figure 4(a) and (b) shows the sol/gel fractions curve and FT-IR spectrum of flexible chain heat curable monomers. 6.0 h is a suitable heat curing time of flexible chain heat curable monomers.

A well oriented planar texture plays a crucial role in the optical performances of prepared CLC composite cells. It is well known that the light scattering phenomenon occurs due to a focal conic texture exhibiting

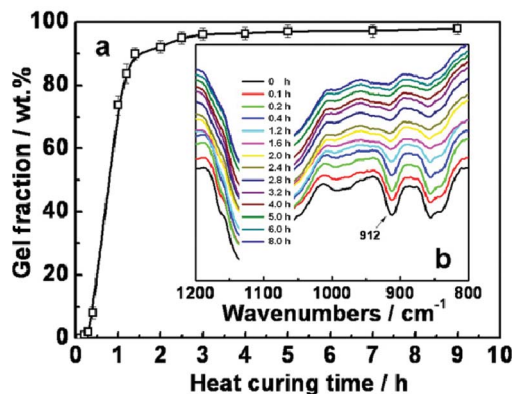


Figure 4. The flexible chain heat curable monomers. (a) The time dependence of gel fractions. (b) FT-IR curves of the reaction.

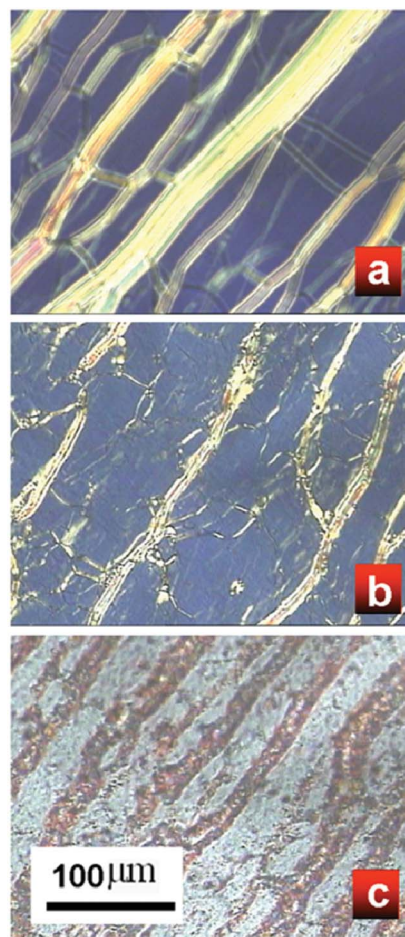


Figure 5. POM photographs of Sample 1 (a) Before UV- and heat curing. (b) After UV-curing but before heat curing. (c) After UV- and heat curing.

polydomains. As shown in Figure 5, the prepared CLC composite has a good planar Grandjean texture before and after UV- and heat curing, so the orientation of the helical axis is not altered by the dual process.

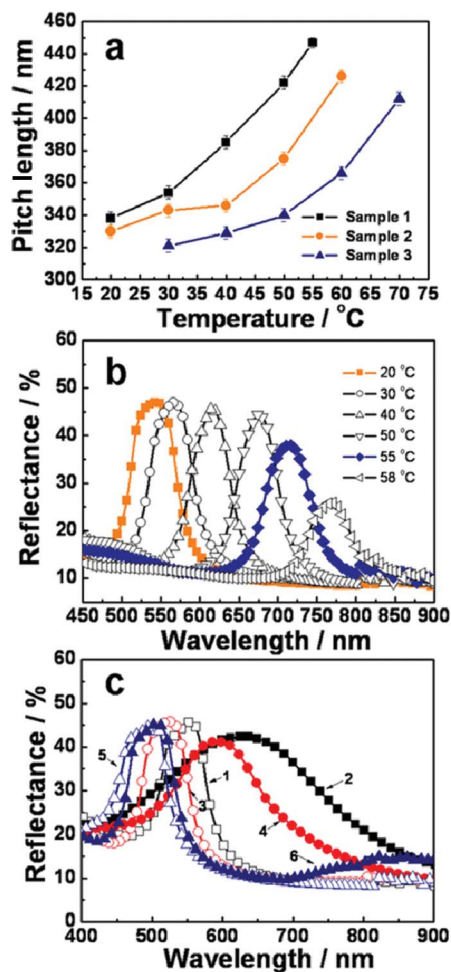


Figure 6. (a) Variation of the helical pitch of Samples 1, 2 and 3 with temperature. (b) The reflection spectrum of Sample 1 shifts to longer wavelength as temperature increases. (c) The reflection spectra of Samples 1, 2 and 3 before polymerisation (curves 1, 3 and 5) and after polymerisation (curves 2, 4 and 6), respectively.

The temperature dependences of the helical pitch for Samples 1, 2 and 3 before polymerisation are shown in Figure 6(a). The helical pitches are measured by the Cano-wedge method [25]. The pitch length of Samples 1, 2 and 3 increases with the increase of temperature. This is due to the fact that the helical twist power (HTP) of the chiral dopant decreases as the temperature increases. Figure 6(b) shows that the reflection spectrum of Sample 1 shifts to longer wavelength with the increase of temperature, measured by a UV/visible/near infrared spectro-photometer. It can be found that the band widths are located in the wavelength of 535, 565, 616, 675, 711 and 769 nm at 20, 30, 40, 50, 55 and 58 °C, respectively. At 58 °C which is close to the shear point, the reflection intensity is only 30%, while at 55 °C it is 40%, so the heat curable temperature at 55 °C is suitable. Figure 6(c) shows

the reflection spectra of Samples 1, 2 and 3 before and after polymerisation, respectively. Because Samples 1, 2 and 3 reflect right-circularly light, the three samples reflect nearly 50% of the incident light before polymerisation, as shown in Figure 6(c) (Curves 1, 3 and 5). Curves 2 and 4 show that the bandwidth of the spectra of Samples 1 and 2 become broadened after both UV- and heat curing. It should be noted that Samples 1 and 2 reflect the visible light flux range of 530–730 nm and 520–640 nm after polymerisation, respectively. The bandwidth of Sample 3 without heat curable monomers makes little change as can be seen from Curve 6, indicating that the reflection locations and bandwidth could hardly be influenced by heat curing. The reflection property of Samples 1 and 2 after curing shows that the distribution of the cholesteric periodicity with long pitch in CLC gel has been frozen during heat curing.

In order to evaluate the influence of cholesteric composites' chemical structure on the polymer network, Figure 7(a) and (b) shows the SEM micrographs of polymer network obtained under heat curing process

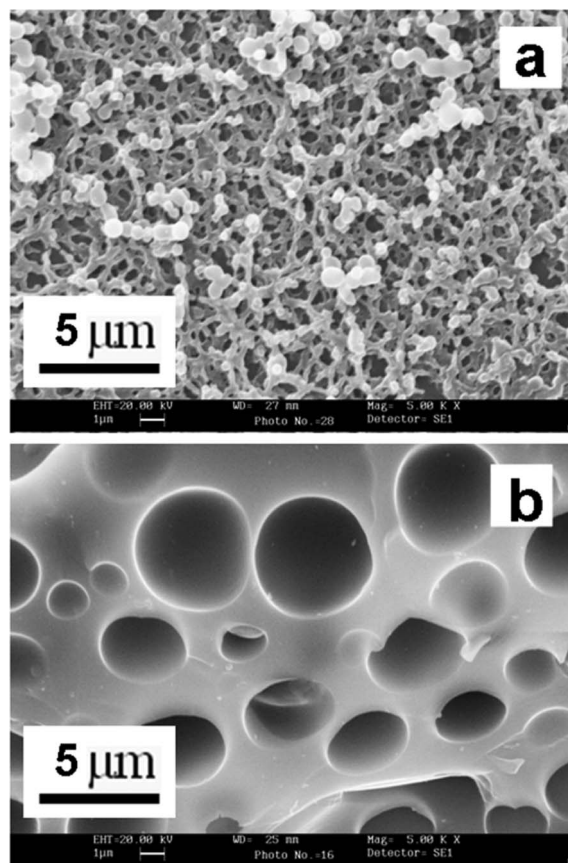


Figure 7. SEM images of the polymer network. (a) Formed by rigid chain heat curable monomers. (b) Formed by flexible chain heat curable monomers.

with rigid chain heat curable monomers and flexible chain ones, respectively. Corresponding to using flexible chain heat curable monomers, rigid chain ones lead to a polymer network with smaller voids. It is often argued that the network morphology is due to the nature of the functional moiety and the flexibility of the chains attached to the mesogenic core. However, there is evidence that smaller voids networks are good for fixing CLCs [26]. The polymer morphology ensures memory effects of the orientational order present when its formation occurs (anisotropic growth of polymer units, for example, oriented fibres). Therefore, the long pitch of CLCs is stabilised easily by the rigid chain heat curing polymer network because of better anchoring effect and the reflective visible light flux range of Sample 1 becomes wider than Sample 2 as can be seen from Figure 6(c) (Curves 2 and 4).

Figure 8(a) provides macroscopic evidence by displaying the photograph of a large-sized homemade cell filled with Samples 1 and 3 step by step. Before polymerisation, greenish and bluish parts represent the mixture of Sample 1 and Sample 3, respectively. The heat curing process was stepped by a sufficient UV-curing procedure. After the reaction finished, the cell was placed under room temperature. Because of the addition of heat curable monomers, the colour of the part corresponding to Sample 1 turned to yellow with a red as shown in Figure 8(b), while the part corresponding to Sample 3 without heat curable monomers remained blue after polymerisation. From the colour changes of the liquid crystal cell we can conclude intuitively that the CLCs with long pitch were fixed by a heat curing network at 55°C. Thus, a colour filter may be prepared via dual UV-light and heat controlling as can be seen from schematic illustration in Figure 8(c).

A conceivable explanation is given considering that anchoring effect of the polymer network and the change of pitch length in cholesteric blend when temperature changes. Figure 9(a) shows the schematic

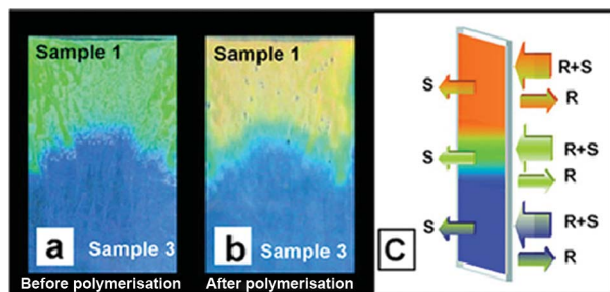


Figure 8. (a) The picture of Samples 1 and 3 before UV- and heat curing. (b) The picture of Samples 1 and 3 after UV- and heat curing. (c) The schematic representation of reflected various visible light colour filter.

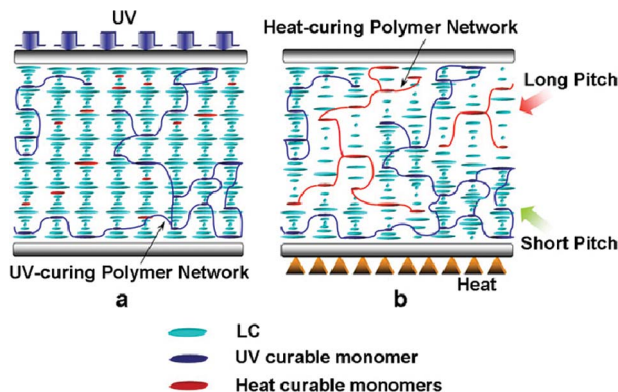


Figure 9. Schematic representation of the arrangement of LC molecules and monomers when the polymerisation conditions change. (a) UV-curing, (b) heat curing.

representation of CLC molecules and the UV-curing polymer network after photo-polymerisation in Samples. In some regions, the alignment of the CLC molecules which are the nearest to the UV-curing polymer network is well stabilised and the rearrangement of CLC molecules with the change of temperature is difficult. Because the HTP of the chiral dopant decreases with the increase of temperature, the pitch length of the blend has tendency to increase as the temperature rises. In some regions, the anchoring effect of the UV-curing polymer network is not enough to prevent the CLC molecules from rearranging. The pitch lengths of the helical structure of the CLC domains in these regions increase with the increase of temperature. At a higher temperature, the heat curing polymer network is formed after heat-polymerisation, as schematically shown in Figure 9(b). After the formation of the heat polymer network, the longer pitch of CLC in the specified regions surrounded by the heat polymer network is frozen. Thus, the cell characteristic that reflects a wide-band is attributed to the CLC composite with various pitches being dispersed in two distinct environments: the UV-curing network-dominated regions and the heat curing network-dominated ones.

4. Conclusions

From the above discussion, it is clear that the bandwidth of the reflection spectrum of the developed composites can be prepared from photo- and thermally-induced processes. By varying the species of heat curable monomers, the reflection bandwidth and its location, in the range of visible region, could be controlled. This result is discussed in relation to the variation of the characteristics of reflection band, which offers an indirect access to the volume distribution of

the cholesteric periodicities. In view of practical applications, broadband reflective cholesteric gels may be of interest for colour filters or for the brightness enhancement films and smart switchable reflective windows.

Acknowledgements

This work was supported by Flat-Panel Display Special Project of China 863 Plan (Grant No. 2008AA03A318), National Natural Science Foundation (Grant No. 50973010), National Natural Science Foundation (Grant No. 20674005) and Projects of Chinese National Science Tackling Key Problems (Grant No. 2007BAE31B02).

References

- [1] Wu, S. T.; Yang, D.K. *Reflective Liquid Crystal Display*; Wiley: Singapore, 2001.
- [2] Ren, H. W.; Wu, S.T. *Appl. Phys. Lett.* **2002**, *81*, 3537–3539.
- [3] Ma, R.Q.; Yang, D.K. *Phys. Rev. E: Stat., Nonlinear, Soft Matter Phys.* **2000**, *61*, 1567–1573.
- [4] Pan, G.H.; Cao, H.; Guo, R.W.; Li, W.B.; Guo, J.B.; Yang, Z.; Huang, W.; He, W.L.; Liang, X.K.; Zhang, D.W.; Yang, H. *Opt. Mater.* **2009**, *31*, 1163–1166.
- [5] Boudet, A.; Binet, C.; Mitov, M.; Bourgerette, C.; Boucher, E. *Eur. Phys. J. E* **2000**, *3*, 247–253.
- [6] Rajaram, C.V.; Hudson, S.D.; Chien, L.C. *Chem. Mater.* **1996**, *8*, 2451–2460.
- [7] Dierking, I. *Adv. Mater.* **2000**, *12*, 167–181.
- [8] Dierking, I.; Kosbar, L.L.; Lowe, A.C.; Held, G.A. *Liq. Cryst.* **1998**, *24*, 387–395.
- [9] Dierking, I.; Kosbar, L.L.; Lowe, A.C.; Held, G.A. *Liq. Cryst.* **1998**, *24*, 397–406.
- [10] Bian, Z.Y.; Li, K.X.; Huang, W.; Cao, H.; Yang, H. *Appl. Phys. Lett.* **2007**, *91*, 201908.
- [11] Xiao, J.M.; Zhao, D.Y.; Cao, H.; Yang, H. *Liq. Cryst.* **2007**, *34*, 473–477.
- [12] Xiao, J.M.; Cao, H.; Yang, H.J. *Appl. Polym. Sci.* **2007**, *105*, 2973–2977.
- [13] Mitov, M.; Dessaud, N. *Nat. Mater.* **2006**, *5*, 361–364.
- [14] Mitov, M.; Dessaud, N. *Liq. Cryst.* **2007**, *34*, 183–193.
- [15] Hikmet, R.A.M.; Kemperman, H. *Nature* **1998**, *392*, 476–479.
- [16] Hikmet, R.A.M.; Polesso, R. *Adv. Mater.* **2002**, *14*, 502–504.
- [17] Relaix, S.; Bourgerette, C.; Mitov, M. *Liq. Cryst.* **2007**, *34*, 1009–1018.
- [18] Relaix, S.; Bourgerette, C.; Mitov, M. *Appl. Phys. Lett.* **2006**, *89*, 251907.
- [19] Broer, D.J.; Lub, J.; Mol, G.N. *Nature* **1995**, *378*, 467–469.
- [20] Broer, D.J.; Mol, G.N. *Adv. Mater.* **1999**, *11*, 573–578.
- [21] Yang, H.; Mishima, K.; Matsuyama, K.; Hayashi, K.I.; Kikuchi, H.; Kajiyama, T. *Appl. Phys. Lett.* **2003**, *82*, 2407.
- [22] Ding, X.K.; Cao, M.; Liu, H.J.; Cao, H.; Li, W.B.; Yang, H. *Liq. Cryst.* **2008**, *35*, 587–595.
- [23] Guo, R.W.; Cao, H.; Liu, H.J.; Li, K.X.; Huang, W.; Xiao, J.M.; Yuan, X.T.; Yang, Z.; Yang, H. *Liq. Cryst.* **2009**, *36*, 939–946.
- [24] Broer, D.J.; Boven, J.; Mol, G.N. *Makromol. Chem.* **1989**, *190*, 2255–2268.
- [25] Cano, R. *Bull. Soc. Fr. Mineral. Cristallogr.* **1968**, *91*, 20–23.
- [26] Guo, J.B.; Sun, J.; Li, K.X.; Cao, H.; Yang, H. *Liq. Cryst.* **2008**, *35*, 87–97.